Cerebellum (2011) 10:88–95
DOI 10.1007/s12311-010-0233-2

ORIGINAL PAPER

Cerebellar Long-term Depression is Deficient in Niemann–Pick Type C Disease Mice

Cheng-Long Sun · Li-Da Su · Qiong Li · Xin-Xin Wang · Ying Shen

Published online: 18 November 2010

Abstract Niemann–Pick type C disease (NPC) is an autosomal recessive lipidosis characterized by progressive neurodegeneration. Although several studies have revealed unusual accumulation of unesterfied cholesterol in astrocytic lysosome of NPC, pathophysiological basis of cerebellar neuronal dysfunction remains unclear. We compared parallel fiber-Purkinje cell synaptic transmission and long-term depression (LTD) in +/+npc^{nih} ($npc^{+/+}$) and −/−npc^{nih} ($npc^{-/-}$) mice. Our data showed that adenosine A1 receptor agonists decreased parallel fiber excitatory postsynaptic current (EPSC) amplitude and mEPSC frequency while its antagonists increased EPSC amplitude and mEPSC frequency in wild type and mutant mice. Furthermore, parallel fiber LTD was deficient in $npc^{-/-}$ mice and supplement of adenosine triphosphate (ATP) rescued the impaired LTD. Taken together, these experiments suggest that synaptic strength and LTD are altered in $npc^{-/-}$ mice due to the decrease of ATP/adenosine release and deactivation of A1 receptors in parallel fiber terminals. The enhanced synaptic transmission and the decreased LTD might result in progressive neurotoxicity of Purkinje cells in $npc^{-/-}$ mice.

Keywords Adenosine · ATP · Purkinje cell · Long-term depression · Cerebellum

Abbreviations

EPSC	Excitatory postsynaptic current
GABA	γ-Aminobutyric acid
LTD	Long-term depression
NPC	Niemann–Pick type C disease
PPF	Paired-pulse facilitation

Introduction

Niemann–Pick type C (NPC) disease is an autosomal degenerative disease [1]. Its clinical symptoms include progressive vertical gaze paralysis, ataxia, dystonia, epilepsy, dementia and dysphonia [2, 3]. A BALB/c mouse model of NPC disease −/−npc^{nih} ($npc^{-/-}$) exhibits neuropathological features similar to the human condition, including cerebral atrophy, demyelination of the corpus callosum and degeneration of cerebellar Purkinje cells [4–9]. It is clear now that this disease is caused by either NPC1 gene mutations (95%) or NPC2 gene mutations (5%) [10–12]. NPC1 mutations leads to abnormal cholesterol accumulation within the lysosomal compartments of astrocytes [13–15], but how such cholesterol accumulation affects brain dysfunction is unknown.

It is recently reported that astrocytic lysosomes contain abundant adenosine triphosphate (ATP), which can be

Electronic supplementary material The online version of this article (doi:10.1007/s12311-010-0233-2) contains supplementary material, which is available to authorized users.

C.-L. Sun · L.-D. Su · Q. Li · X.-X. Wang · Y. Shen (✉)
Department of Neurobiology, Key Laboratory of Medical Neurobiology of Ministry of Health of China, Zhejiang Province Key Laboratory of Neurobiology, Zhejiang University School of Medicine,
388 YuHangTang Rd,
Hangzhou, Zhejiang 310058, People's Republic of China
e-mail: yshen@zju.edu.cn

L.-D. Su
Neuroscience Care Unit, The Second Affiliated Hospital of Zhejiang University School of Medicine,
Hangzhou, Zhejiang, People's Republic of China

released in a stimulus-dependent manner in cultured hippocampal astrocytes [16]. In addition, earlier studies have suggested that ATP and adenosine suppress synaptic networks through presynaptic modulation of [17–19]. Thus, a reasonable hypothesis that explains how NPC1 mutations-induced cholesterol accumulation in astrocytic lysosomes affects brain function is that cholesterol accumulation decreases ATP/adenosine synthesis and release and consequently affect synaptic functions.

We set out to test this hypothesis in $npc^{-/-}$ mice. Although Purkinje cell degeneration has been observed in $npc^{-/-}$ mice [7, 19, 20], it is unknown as to whether change of ATP/adenosine release causes Purkinje cell dysfunction. In the present study, by using slice whole-cell patch-clamp combined with pharmacological applications, we aimed to compare parallel fiber-Purkinje cell synaptic transmission and long-term depression (LTD) in the wild type (+/+npc^{nih}, $npc^{+/+}$) and $npc^{-/-}$ mice. Our results show that synaptic transmission was increased and LTD was blocked in $npc^{-/-}$ parallel fiber-Purkinje cell synapse, suggesting a potential mechanism through which Purkinje cells are more vulnerable in $npc^{-/-}$ mice.

Materials and Methods

All animal experiments were performed under the guidance of National Institute of Health (USA) regarding the care and use of animals and, approved by Animal Experimentation Ethics Committee of Zhejiang University and specifically designed to minimize the number of animals. Mice that were $npc^{+/+}$, $npc^{+/-}$, or $npc^{-/-}$ with respect to the *NPC1* gene mutation [10, 11] were obtained from an established breeding colony of npc^{nih} mice at the Experimental Animal Center of Zhejiang University School of Medicine (original breeding pairs were provided courtesy of Dr. ShuMin Duan, Institute of Neuroscience, Chinese Academy of Sciences, Shanghai, People's Republic of China). Mice were maintained under temperature-controlled conditions on a 12:12 h light/dark cycle with food and water ad libitum. The genotype of individual animal was determined from genomic DNA isolated from a small piece of the tail, using minor modifications of the polymerase chain reaction (PCR)-based method and oligonucleotide primers described in previous work [11]. Specifically, after 0.5 cm pieces of tail tissue were incubated overnight at 55°C in 500 μl of lysis buffer (100 mM Tris, 5 mM EDTA, 0.2% SDS, and 20 mM NaCl) containing 10 μl of 10 mg/ml proteinase K, 5 μl aliquots of the supernatants were incubated with 3.5 pmol of forward (5′-GGTGCTGGACAGCCA AGTA-3′) and reverse (5′-GAT GGTCTGTTCTCCCATG-3′) primers for 5 min at 94°C and for 30 PCR cycles (94°C for 1 min, 55°C for 2 min, and 72°C for 3 min). PCR products were used to determine the genotype (173 bp for $npc^{+/+}$, 475 bp for $npc^{-/-}$, and products of both sizes for $npc^{+/-}$ mice), as shown in Fig. 3a. The percentage of postnatal $npc^{-/-}$ mice (12% of total 200 littermates) was similar to previous report [21].

The electrophysiological experiments used here were modified from those in previous work [22, 23]. Parasagittal slices of the cerebellar vermis (250 μM) were prepared from P17–23 mice using a vibrating tissue slicer (Leica VT1000S, Germany) and ice-cold standard artificial cerebrospinal fluid (ACSF) containing (in mM): 124 NaCl, 5 KCl, 1.25 NaH_2PO_4, 2 $MgSO_4$, 2 $CaCl_2$, 26 $NaHCO_3$ and 10 D-glucose, bubbled with 95 O_2 and 5% CO_2. After a recovery period of 30 min at 37°C, the slices were placed in a submerged chamber that was perfused at 2 ml/min with ACSF supplemented with 10 μM GABAzine to block $GABA_A$ receptors. The recording electrodes were filled with a solution containing (in mM): 135 CsMes, 10 CsCl, 10 HEPES, 4 Na_2ATP, 0.4 Na_3GTP, and 0.3 EGTA (pH 7.2). Resistances of recording pipettes were typically 1.5–3 MΩ, and uncompensated series resistances were less than 5 MΩ.

Purkinje cells were visualized using an upright Olympus BX51 (Olympus Optical, Tokyo, Japan) with a 40× water immersion objective and equipped with infrared-differential interference contrast enhancement. We selected Purkinje cells in lobule V for recording throughout experiments to avoid regional cholesterol difference. Whole-cell recordings were obtained with an Axopatch 200B amplifier (Molecular Devices, Foster City, CA). Currents were filtered at 1 kHz and digitized at 10 kHz. For parallel fiber stimulation, standard patch pipettes were filled with ACSF and placed in the middle third of the molecular layer. Synaptic responses were evoked every 20 s using 12–16 μA pulses (100 μs duration). When burst stimulation was employed, the interpulse interval was set as 10 ms. Paired-pulse facilitation protocol was employed to measure peak amplitudes of two consecutive EPSCs, separated by a inter-stimulus interval of 30 ms. The average of three to five trials was used to calculate the percentage facilitation $(100\times(A2–A1)/A1)$, where *A1* and *A2* were the average peak amplitude of the first (EPSC1) and second EPSC, respectively, in response to a single stimulation. Purkinje cell miniature EPSCs (mEPSCs) were recorded in whole-cell configuration in the presence of 0.5 μM tetrodotoxin (TTX) to block evoked synaptic transmission and GABAzine to suppress spontaneous IPSCs. mEPSCs offline analysis was conducted using a sliding template algorithm (ClampFit 10, Molecular Device) [24]. The criteria for inclusion were a 6 pA amplitude threshold and a rise time (10–90%) longer than 1 ms. Overlapping events were rejected.

All drugs were purchased from Sigma (St. Louis, MO) unless stated otherwise. Data analysis was performed using

Excel 2003 (Microsoft, Chicago, IL), Clampfit 10 and Igor Pro 6.0 (Wavemetrics, Lake Oswego, OR). All group data are shown as mean±SEM. Student's *t* tests were used to determine *p* values. *n* represents numbers of cells used in each experiment derived from at least three animals. Cells were excluded from the study if series resistance or input resistance varied by more than 15% over the course of an experiment.

Results

Effects of ATP and CPT in Parallel Fiber-Purkinje Cell synapse

Previous studies have shown that extracellular adenosine tonically inhibits the synaptic transmission by activating adenosine A1 receptors and modulating presynaptic calcium channels on parallel fibers [17, 18, 25]. To address if synaptic transmission is controlled by the A1 receptor activation in parallel fiber-Purkinje cell synapse, we examined the EPSC amplitude and paired-pulse facilitation (PPF) in $npc^{+/+}$ and $npc^{-/-}$ mice. We first quantified effects of external 100 μM ATP, an A1 receptor agonist, or 200 nM carnitine palmitoyltransferase (CPT), an A1 receptor antagonist, or both on parallel fiber EPSCs in $npc^{+/+}$ Purkinje cells. While ATP dramatically decreased EPSC1 (22.9±5.4% of baseline; n=12; Fig. 1a), CPT slightly increased EPSC1 (132.9±5.4% of baseline; n=12; Fig. 1b). ATP and CPT exerted opposite effects on the parallel fiber EPSC PPF. While ATP significantly increased the PPF from 186.9±13.4% (before) to 330.5±14.5% (after; n=12), CPT decreased the PPF from 190.3±11.4% (before) to 147.5±8.5% (after; n=12). Since ATP bounds to P2X receptors in parallel fibers as well [26], one may argue that ATP may not only work on A1 receptors. To address this concern, we co-applied 100 μM ATP and 200 nM CPT after a baseline recording in $npc^{+/+}$ slices. ATP+CPT decreased EPSC1 amplitude (47.5±5.5% of baseline; n=11; Fig. 1c), which was much smaller than that in the ATP alone. There was no significant PPF change before and after co-application of ATP and CPT (before, 182.3±6.4%; after, 211.1±9.3%; n=11). Likewise, we observed effects of 100 μM ATP or 200 nM CPT in $npc^{-/-}$ Purkinje cells. We found that the EPSC1 decreased (26.5±7.5% of baseline) and the PPF increased (before, 147.7±12.1%; after, 286.5±18.3%; n=22; Fig. 1d) after the ATP application, similar to the result of $npc^{+/+}$ Purkinje cells (Fig. 1a). However, adding CPT in external saline did not exert any significant action on the EPSC1 amplitude (95.5±6.5% of baseline) and PPF (before, 138.3±9.4%; after, 133.9±9.9%; n=10; Fig. 1e). We also observed effects of 100 μM adenosine (agonist) and 200 nM DPCPX (antagonist) in $npc^{+/+}$ Purkinje cells. As shown in the Electronic Supplementary Material (Fig. S1), similar results were found for changes of EPSC1 amplitude and PPF.

To further confirm the roles of A1 receptor activation on parallel fiber-Purkinje cell synaptic transmission, we recorded mEPSCs by holding the Purkinje cells at a command potential of −70 mV in the external saline supplemented with TTX and GABAzine; 0.5 μM DCG IV (a group II mGluR agonist) was also added to suppress climbing fiber mEPSC [27]. Following a stabilization period (>10 min), we recorded mEPSCs for >15 minutes with different pharmacologic treatments. Representative recordings are shown in Figs. 2a, b. In $npc^{+/+}$ cells, the mean control frequency and amplitude were 1.4±0.1 Hz and 12.4±0.8 pA, respectively (n=10). ATP reduced the mEPSC frequency to 0.9±0.1 Hz. In marked contrast, CPT increased the mean mIPSC frequency to 2.0±0.3 Hz. Neither ATP nor CPT changed mEPSC amplitudes (11.4±0.8 pA and 12.0±0.9 pA, respectively). We repeated mEPSC recordings in $npc^{-/-}$ cells where the mean control frequency and amplitude were 2.1±0.2 Hz and 12.5±1.0 pA, respectively (n=11). Subsequent ATP application decreased the mEPSC frequency to 0.9±0.1 Hz. Conversely, CPT did not significantly change the frequency (2.4±0.2 Hz). Similar to $npc^{+/+}$ cells, ATP and CPT did not change the mEPSC amplitude (11.0±0.7 pA and 10.8±1.1 pA, respectively). The ATP and CPT effects could be washed out completely. These data suggested that ATP may inhibit the synaptic transmission by activating presynaptic A1 receptors.

Parallel Fiber-Purkinje Cell LTD is Deficient in $npc^{-/-}$ Mice

We then determined whether synaptic plasticity was changed in $npc^{-/-}$ cerebellum. Test responses to the parallel fiber stimulation were monitored in voltage-clamp mode, as shown by representative traces in Fig. 3b. Following a 10-min-baseline-recording period, parallel fibers were tetanized with a train of 5 pulses at 100 Hz, which was accompanied by a 100-ms-long depolarization to 0 mV in the Purkinje cell [22, 23]. These bursts were repeated 30 times with an interburst interval of 2 s. After tetanus stimuli, slices from the $npc^{+/+}$ group showed robust LTD (45.6±4.0% of baseline at t=30 min; n=8; Fig. 3c), while the LTD could not be induced in $npc^{-/-}$ mice (98.5±3.8% of baseline at t=30 min, n=10; P<0.01). Thus, the parallel fiber-Purkinje cell synaptic LTD was deficient in $npc^{-/-}$ mice.

Roles of ATP and CPT on LTD Induction

We further examined the functions of A1 receptors in parallel fiber LTD by pharmacological treatment and

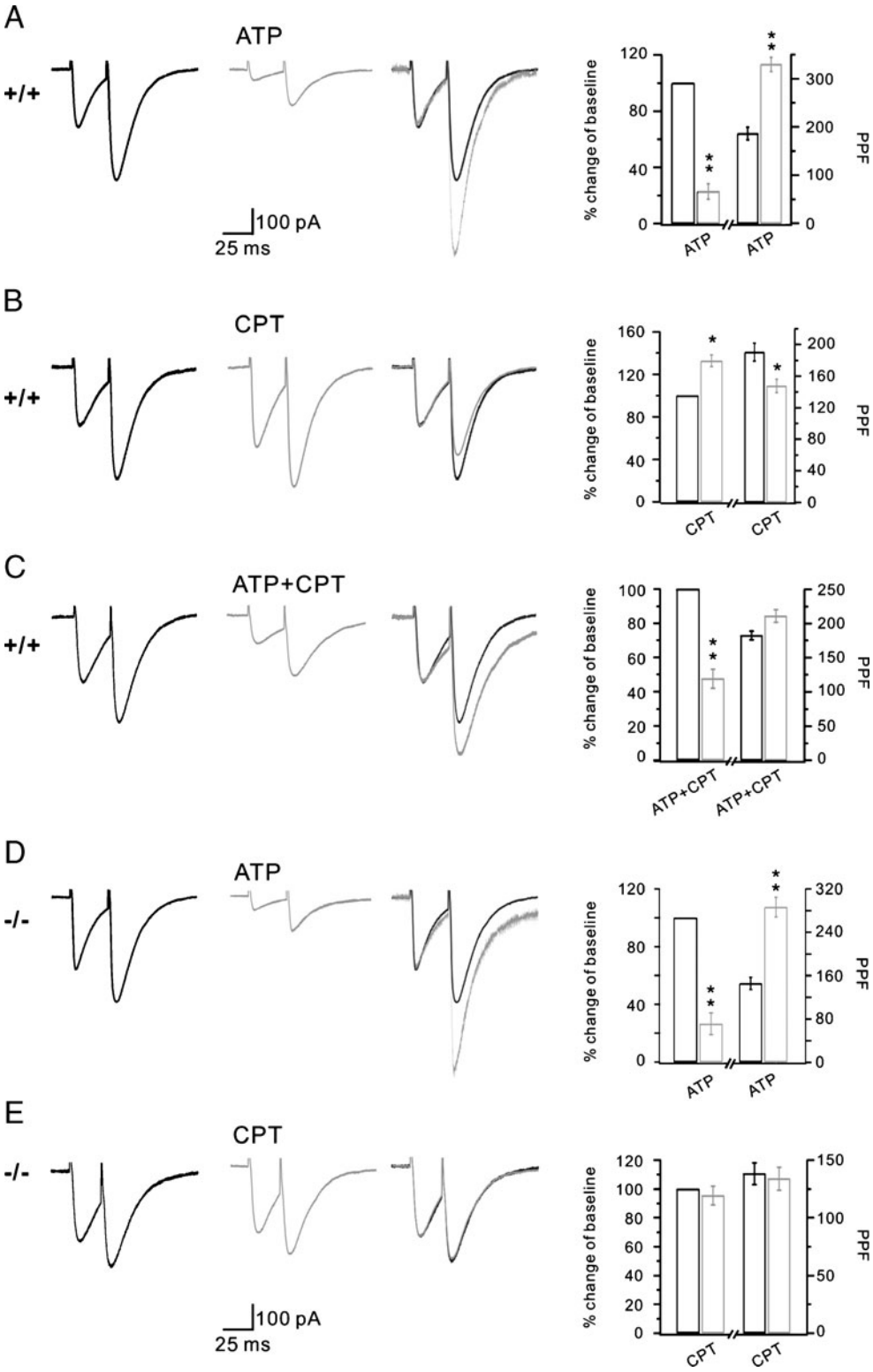

Fig. 1 Adenosine A1 receptor inhibition increases synaptic strength in parallel fiber-Purkinje cell synapse. **a**–**c** Representative responses evoked by paired-pulse parallel fiber stimuli from three individual $npc^{+/+}$ Purkinje cells. EPSCs before and after compound applications are shown in *black* and *grey*, respectively. For comparison, *grey traces* are normalized to their corresponding *black traces* according to the amplitude of EPSC1 and superimposed on *black traces*. Statistics of EPSC1 amplitude and PPF after ATP, CPT or ATP+CPT applications are shown in the bar graphs. **d**, **e** Representative responses evoked by paired-pulse stimuli from two $npc^{-/-}$ individual Purkinje cells (*black traces*). EPSCs after ATP or CPT applications are shown in grey and normalized to *black traces* according to the peak of EPSC1 and superimposed together for comparison. Statistics are shown in the *bar graphs*. **P*<0.05; ***P*<0.01, *t* test. *Error bars* represent SEM

genetic manipulation. Slices derived from $npc^{+/+}$ and $npc^{-/-}$ littermates were incubated with 200 nM CPT for 30 min prior to recordings. As a control, 0.002% DMSO was incubated in slices to exclude potential toxic effects of solvent. Parallel fiber LTD induction was conducted in Purkinje cells. Figure 4a shows the representative parallel fiber EPSCs recorded before and after LTD induction. In $npc^{+/+}$ mice, LTD was induced in DMSO (56.5±4.8% of baseline at t=30 min; n=10), but was partially suppressed after 200 nM CPT incubation (81.5±4.7% of baseline at

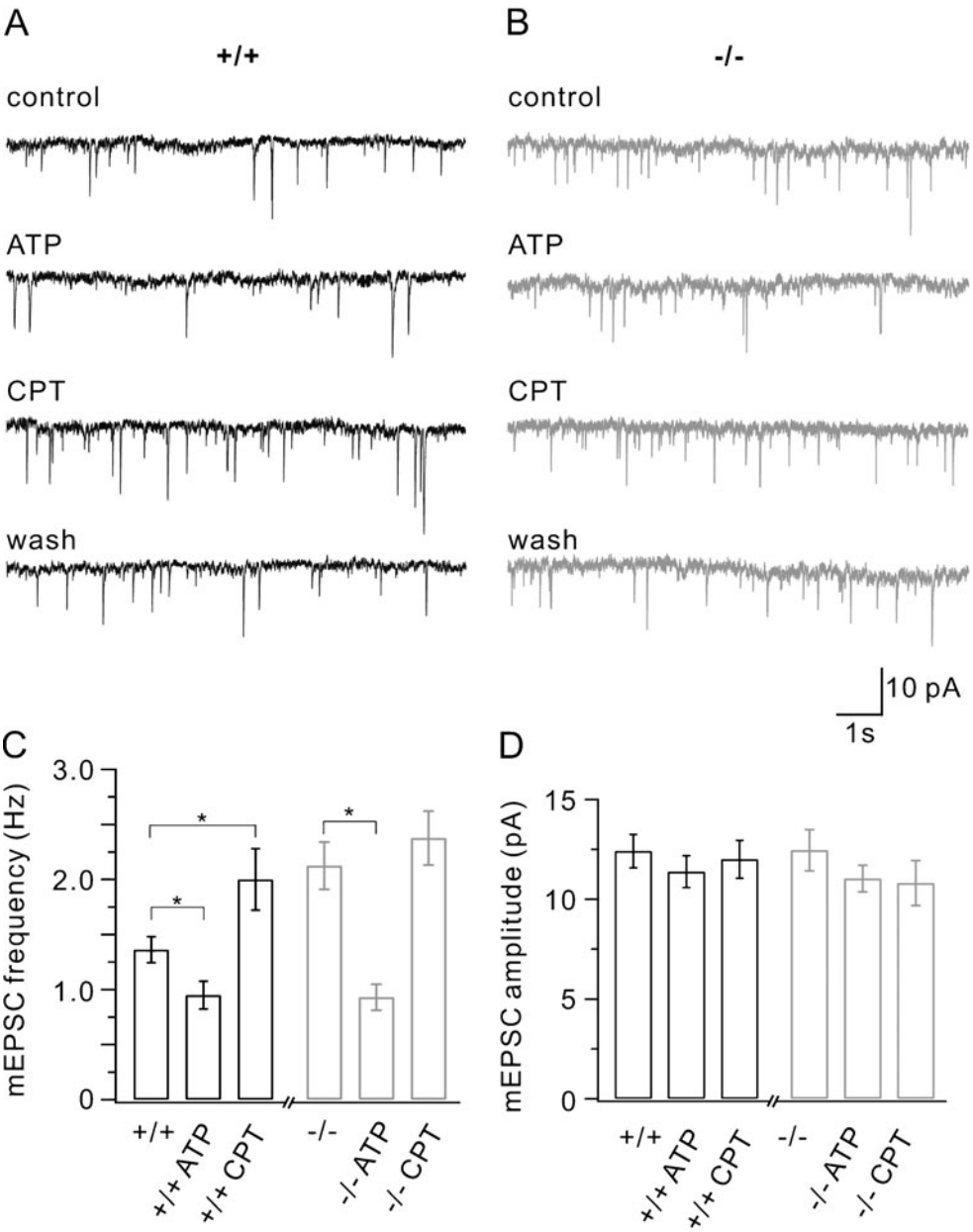

Fig. 2 Purkinje cell mEPSCs. **a** mEPSCs recorded from one "+/+" Purkinje cell. *Top trace*, in control saline (control); *second trace*, 2 min after exposure to 100 mM adenosine triphosphate (*ATP*); *third trace*, 2 min after exposure to 1 mM carnitine palmitoyltransferase (*CPT*); *bottom trace*, 4 min after wash-out (wash). **b** mEPSCs obtained from one "−/−" Purkinje cell. *Top trace*, in control saline (control); *second trace*, 2 min after exposure to 100 mM ATP; *third trace*, 2 min after exposure to 1 mM CPT; *bottom trace*, 4 min after wash-out (wash). "+/+" and "−/−" represent $npc^{+/+}$ and $npc^{-/-}$, respectively. **c** Summary of mEPSC frequencies in various experimental conditions. *$P<0.05$, *t* test. **d** Summary of mEPSC amplitudes in different conditions. *Error bars* represent SEM

$t=30$ min; $n=10$; $P<0.01$ compared with group "+/+ DMSO"). In $npc^{-/-}$ slices, LTD was failed to be induced after the incubation of 0.002% DMSO. With an average EPSC amplitude of 90.3±4.6% of baseline ($n=10$), additional 200 nM CPT in external saline did not further suppress the EPSC amplitudes (88.4±8.8% of baseline; $n=10$; $P>0.05$ compared with group "−/− DMSO"). If parallel LTD was blocked in $npc^{-/-}$ mice, one might propose that the activation of A1 receptors might rescue the LTD. We then incubate $npc^{-/-}$ slices with 1 μM ATP for 30 minutes prior to recordings and maintain it during the experiments. With EPSC amplitude slightly decreased, 1 μM ATP rescued parallel fiber LTD in the $npc^{-/-}$ Purkinje cells (67.2±8.3% of baseline at $t=30$ min; $n=8$; $P<0.01$ compared with group "−/− DMSO"). These data suggest that adenosine A1 receptor inhibition was sufficient to block parallel fiber-Purkinje cell LTD.

Discussion

The main finding of the present study was that the parallel fiber-Purkinje cell synaptic transmission was enhanced and the LTD was deficient in postnatal 3-week-old $npc^{-/-}$ mice. Experiments with ATP and CPT applications indicated that the synaptic transmission was increased by inhibiting presynaptic A1 receptors or decreasing the ATP/adenosine in the NPC1 ablation mice (Figs. 1 and 2; also see the Electronic Supplementary Material, Fig. S1). This enhanced glutamatergic synaptic transmission then led to the im-

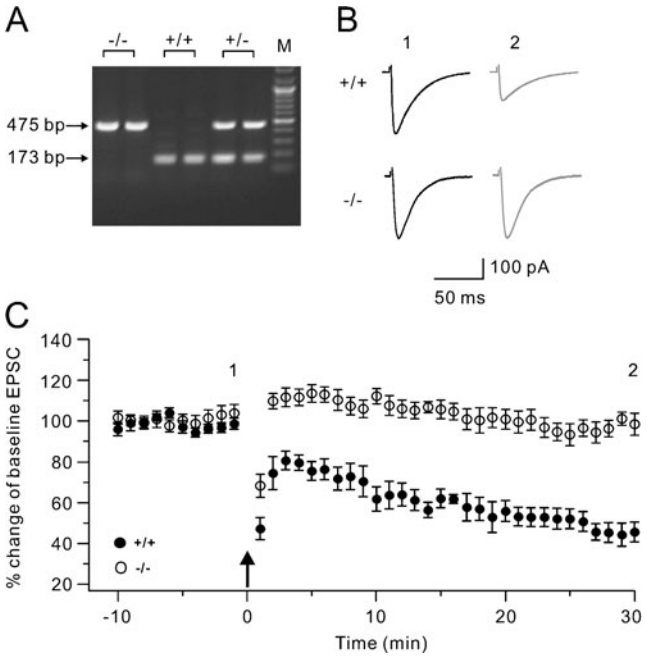

Fig. 3 Parallel fiber-Purkinje cell LTD is deficient in $npc^{-/-}$ mice. **a** PCR detection of NPC1 mRNA expression. Tail RNA from $npc^{-/-}$ (−/−), $npc^{+/+}$ (+/+) and $npc^{+/-}$ (+/−) are shown by *lanes from left to right*. *M* marker. **b** Representative parallel fiber EPSCs from "+/+" or "−/−" cells at the time points indicated in (**c**). "+/+" and "−/−" represent $npc^{+/+}$ and $npc^{-/-}$, respectively. To present LTD, a time course of percentage changes of EPSC amplitudes is shown in (**c**), which is a population of parallel fiber-Purkinje cell EPSCs derived from "+/+" (*filled circles*) or "−/−" (*empty circles*). Tetanic stimulation is indicated by an *upward arrow*

paired parallel fiber-Purkinje cell LTD (Fig. 3). This LTD impairment was due to the deactivation of A1 receptors because the pre-incubation of A1 receptor antagonist, CPT, suppressed the LTD in $npc^{+/+}$ and $npc^{-/-}$ Purkinje cells (Fig. 4). Interestingly, supplemental ATP could rescue the parallel fiber LTD in NPC mice (Fig. 4). Taken together, these experiments provide the first line of evidence supporting that cerebellar synaptic transmission and plasticity are defective in $npc^{-/-}$ mice. Although we did not provide the direct evidence in this study that NPC1 deletion results in apparent Purkinje cell neurodegeneration, it might be hypothesized that the increased excitatory neurotransmission and LTD deficiency lead to chronic Purkinje cell excitotoxicity.

Adenosine A1 receptors are broadly expressed in most brain regions and play important roles in modulating the neurotransmitter release and neuronal excitability [16, 28–30]. In line with previous work [17–19, 25], we showed that A1 receptor activation affects AMPA receptor-mediated parallel fiber EPSC and PPF. Moreover, the deactivation of A1 receptors blocked parallel fiber LTD and interestingly, the activation of A1 receptors by small amount of ATP could rescue the LTD in $npc^{-/-}$ Purkinje cells. These data suggested that the mild presynaptic inhibition of glutamate release by A1 receptors is critical to LTD induction at parallel fiber-Purkinje cell synapses. Excessive glutamate in synaptic cleft not only produces neurotoxicity but also decreases the postsynaptic sensitivity to LTD induction due to the regulated strength of basal transmission. It was also reported that the activation of adenosine receptors modulates GABA receptors in granule cells [31] and metabotropic

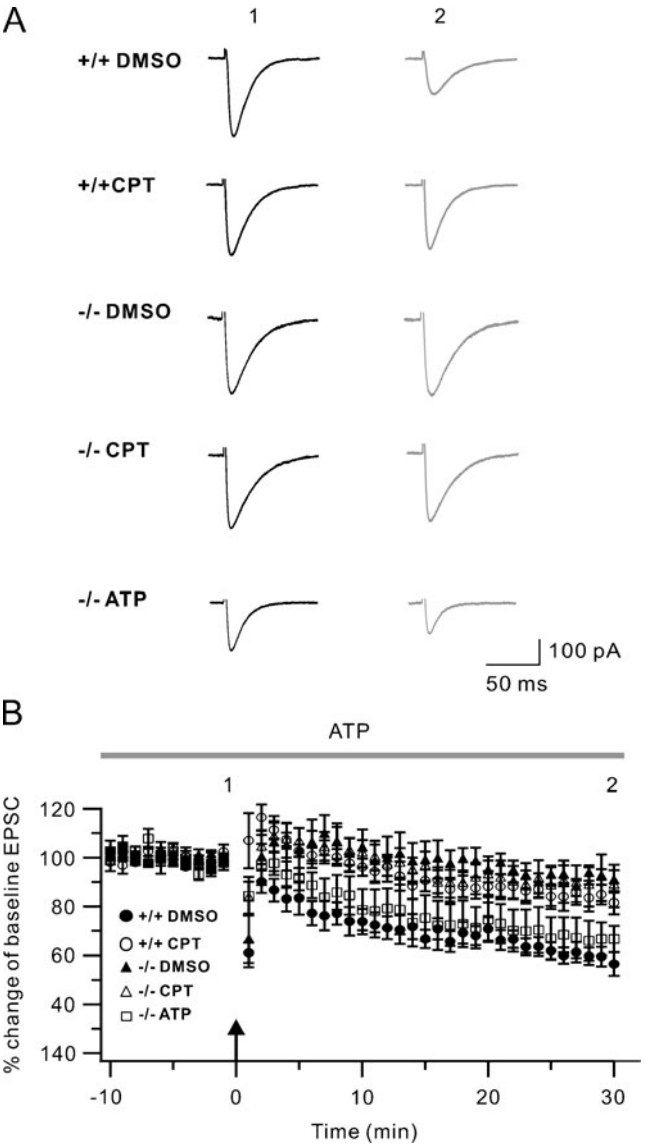

Fig. 4 Roles of ATP and CPT in parallel fiber LTD. **a** Representative traces of parallel fiber EPSC at the time points indicated in (**b**). Experimental conditions are labeled in the left as "+/+ DMSO", "+/+ CPT", "−/− DMSO", "−/− CPT" or "−/− ATP". "+/+" and "−/−" represent $npc^{+/+}$ and $npc^{-/-}$, respectively. **b** The time course of percentage changes of EPSC amplitudes for populations of Purkinje cells indicated by "+/+ DMSO, *filled circles*"; "+/+ CPT, *empty circles*"; "−/− DMSO, *filled triangles*"; "−/− CPT, *empty triangles*" or "−/− ATP, *empty squares*". For "−/− ATP" group experiments, ATP was introduced 30 min prior to recording and maintained during the experiments, as indicated by the *grey bar* in (**b**). Tetanic stimulation is indicated by an *upward arrow*

glutamate receptors in cultured Purkinje cells ([32]; also see Kamikubo et al., 2009 SFN abstract 320.11/C61). These findings suggest that adenosine may exert the complicated effects on synaptic and cellular activities.

Although the mechanisms underlying the decreased extracellular adenosine in $npc^{-/-}$ mice are not clear, several studies suggest that defective lysomal exocytosis might be involved. The NPC1 protein is predominantly present in astrocytic processes closely associated with nerve terminals [33]. Mutation in the NPC1 protein causes deficiency of lysosomal transport of cholesterol, glycolipids, and other molecules [11, 34]. Zhang et al. found that astrocytic lysosomes contain abundant ATP that can be released *via* the lysosome exocytosis [16]. Extracellular adenosine in the brain is mainly derived from the degradation of ATP [26, 28, 35]. Adenosine is responsible for tonic and activity-induced presynaptic suppression [28, 30]. It thus seems likely that excessive accumulated cholesterol in the endosomal/lysosomal in $npc^{-/-}$ astrocytes impairs lysosomal fusion with the plasma membrane, thereby impairing the ATP exocytosis.

Direct evidence of extracellular adenosine in the immature [36] and the mature cerebellum [19], as measureed with biosensors, has been missing. In contrast, extracellular adenosine is present in acute hippocampal slices and decreases in $npc^{-/-}$ mice [37]. Future work is needed to determine whether or not ATP and adenosine are present in the cerebellum. It is also possible that, even though ATP and adenosine are absent in normal cerebellum, ATP can be released from glia cells after tetanus stimuli or under some pathological conditions.

NPC patients generally suffer from increasing neuronal degeneration [2, 3]. Similar to NPC patients, $npc^{-/-}$ mice show metabolic disorders and mental defects in behavior [5, 7, 8]. Seven-week-old $npc^{-/-}$ mice show a deficit in consolidation and retrieval of the learned spatial information in water maze tests [1]. In the cerebellum, abnormal axonal vesicles appear in Purkinje cells and granule cells in 4-week-old $npc^{-/-}$ mice. Particularly, Purkinje cells bear abnormal morphology and functional activities and begin to die quickly after postnatal 11 weeks [7] when motor tasks are impaired [8]. While the present work suggests that $npc^{-/-}$ Purkinje cells may suffer more neurotoxicity due to the increased excitatory neurotransmission and the LTD deficiency, it remains to be determined whether the symptomatic loss of Purkinje cells corresponds to this chronically altered synaptic transmission and its-induced neurotoxicity.

Conclusions

Although pathological studies have revealed abnormal accumulation of unesterfied cholesterol in $npc^{-/-}$ astrocytic lysosome, it is yet unclear how this accumulation affects synaptic transmission and neuronal dysfunction in the cerebellum. In the present study, we found that pharmacological treatments with ATP and CPT altered parallel fiber synaptic transmission in $npc^{+/+}$ and $npc^{-/-}$ mice. Deletion of the NPC1 gene resulted in blockade of parallel fiber-Purkinje cell LTD, which could be mimicked by deactivation of A1 receptors. Furthermore, supplement of ATP rescued the impaired LTD in mutant mice. In summary, we have showed that NPC1 gene deletion causes elevated excitatory synaptic transmission and LTD induction failure at parallel fiber-Purkinje cell synapses.

Acknowledgments We are grateful for helpful comments from members of Shen laboratory. We thank Drs. Jun Xia, Su-Ya Zhou and Jian-Hong Luo for helpful discussion. This work was supported by grants from the National Foundation of Natural Science of China (No. 30600168, to Y. S.), Zhejiang Provincial Foundation of Natural Science (No. R206018, to Y. S. and N_HKUST605/07, to J. X.), the National Foundation of Natural Science of China/Hong Kong Research Grants Council JRS fund (No. 30731160616, to Y. S.), the New Century Talent Award of the Ministry of Education of China (No. NCET-07-0751, to Y. S.) and the National Basic Research Program (Project 973) of the Ministry of Science and Technology of China (No. 2009CB94140 and 2011CB5044000).

References

1. Pentchev PG, Vanier MT, Suzuki K, Patterson MC. Niemann–Pick disease type C: a cellular cholesterol lipidosis. In: Scriver CR, Beaudet AL, Sly WS, Valle D, editors. The metabolic and molecular basis of inherited disease. 7th ed. New York: McGraw-Hill; 1995. p. 2625–39.
2. Vanier MT, Millat G. Niemann–Pick disease type C. Clin Genet. 2003;64:269–81.
3. Sevin M, Lesca G, Baumann N, Millat G, Lyon-Caen O, Vanier MT, et al. The adult form of Niemann–Pick disease type C. Brain. 2007;130:120–33.
4. Pentchev PG, Comly ME, Kruth HS, Vanier MT, Wenger DA, Patel S, et al. A defect in cholesterol esterification in Niemann–Pick disease (type C) patients. Proc Natl Acad Sci USA. 1985;82:8247–51.
5. Higashi Y, Murayama S, Pentchev PG, Suzuki K. Cerebellar degeneration in the Niemann–Pick type C mouse. Acta Neuropathol. 1993;85:175–84.
6. Akaboshi S, Yano T, Miyawaki S, Ohno K, Takeshita K. A C57BL/KsJ mouse model of Niemann–Pick disease (spm) belongs to the same complementation group as the major childhood type of Niemann–Pick disease type C. Hum Genet. 1997;99:350–3.
7. German DC, Quintero EM, Liang C, Xie C, Dietschy JM. Degeneration of neurons and glia in the Niemann–Pick C mouse is unrelated to the low-density lipoprotein receptor. Neurosci. 2001;105:999–1005.
8. Võikar V, Rauvala H, Ikonen E. Cognitive deficit and development of motor impairment in a mouse model of Niemann–Pick type C disease. Behav Brain Res. 2002;132:1–10.
9. Amritraj A, Peake K, Kodam A, Salio C, Merighi A, Vance JE, et al. Increased activity and altered subcellular distribution of lysosomal enzymes determine neuronal vulnerability in Niemann–Pick type C1-deficient mice. Am J Pathol. 2009;175:2540–56.

10. Carstea ED, Morris JA, Coleman KG, Loftus SK, Zhang D, Cummings C, et al. Niemann–Pick C1 disease gene: homology to mediators of cholesterol homeostasis. Science. 1997;277:228–31.
11. Loftus SK, Morris JA, Carstea ED, Gu JZ, Cummings C, Brown A, et al. Murine model of Niemann–Pick C disease: mutation in a cholesterol homeostasis gene. Science. 1997;277:232–5.
12. Naureckiene S, Sleat DE, Lackland H, Fensom A, Vanier MT, Wattiaux R, et al. Identification of HE1 as the second gene of Niemann–Pick C disease. Science. 2000;290:2298–301.
13. Patel SC, Asotra K, Patel YC, Patel RC, Suresh S. 25-Hydroxycholesterol induces reorganization of lysosomes in normal but not Niemann–Pick disease type C astrocytes. NeuroReport. 1994;5:2121–4.
14. Patel SC, Suresh S, Kumar U, Hu CY, Cooney A, Blanchette-Mackie EJ, et al. Localization of Niemann–Pick C1 protein in astrocytes: implications for neuronal degeneration in Niemann–Pick type C disease. Proc Natl Acad Sci USA. 1999;96:1657–62.
15. Paul CA, Boegle AK, Maue RA. Before the loss: neuronal dysfunction in Niemann–Pick Type C disease. Biochem Biophys Acta. 2004;1685:63–76.
16. Zhang Z, Chen G, Zhou W, Song A, Xu T, Luo Q, et al. Regulated ATP release from astrocytes through lysosome exocytosis. Nat Cell Biol. 2007;9:945–53.
17. Takahashi M, Kovalchuk Y, Atwell D. Pre- and postsynaptic determinants of EPSC waveform at cerebellar fiber and parallel fiber to Purkinje cell synapses. J Neurosci. 1995;15:5693–702.
18. Dittman JS, Regehr WG. Contributions of calcium-dependent and calcium-independent mechanisms to presynaptic inhibition at a cerebellar synapse. J Neurosci. 1996;16:1623–33.
19. Wall MJ, Atterbury A, Dale N. Control of basal extracellular adenosine concentration in rat cerebellum. J Physiol. 2007;582:137–51.
20. Tanaka J, Nakamura H, Miyawaki S. Cerebellar involvement in murine sphingomyelinosis: a new model of Niemann–Pick disease. J Neuropathol Exp Neurol. 1988;47:291–300.
21. Henderson LP, Lin L, Prasad A, Paul CA, Chang TY, Maue RA. Embryonic striatal neurons from Niemann–Pick Type C mice exhibit defects in cholesterol metabolism and neurotrophin responsiveness. J Biol Chem. 2000;275:20179–87.
22. Steinberg JP, Takamiya K, Shen Y, Xia J, Rubio ME, Yu S, et al. Targeted in vivo mutations of the AMPA receptor subunits GluR2 and its interacting protein PICK1 eliminate cerebellar long-term depression. Neuron. 2006;49:845–86.
23. Su LD, Sun CL, Shen Y. Ethanol acutely modulates mGluR1-dependent long-term depression in cerebellum. Alcohol Clin Exp Res. 2010;34:1140–5.
24. Ramanan N, Shen Y, Sarsfield SL, Linden DJ, Ginty DD. Distinct requirements for SRF and CREB in neuronal survival and synaptic plasticity. Nat Neurosci. 2005;8:759–67.
25. Kocsis JD, Eng DL, Bhisitkul RB. Adenosine selectively blocks parallel-fiber-mediated synaptic potentials in rat cerebellar cortex. Proc Natl Acad Sci USA. 1984;81:6531–4.
26. Rubio ME, Soto F. Distinct Localization of P2X receptors at excitatory postsynaptic specializations. J Neurosci. 2001;21:641–53.
27. Maejima T, Hashimoto K, Yoshida T, Aiba A, Kano M. Presynaptic inhibition caused by retrograde signal from metabotropic glutamate to cannabinoid receptors. Neuron. 2001;31:463–75.
28. Zhang JM, Wang HK, Ye CQ, Ge W, Chen Y, Jiang ZL, et al. ATP released by astrocytes mediates glutamatergic activity-dependent heterosynaptic suppression. Neuron. 2003;40:971–82.
29. Brambilla D, Chapman D, Greene R. Adenosine mediation of presynaptic feedback inhibition of glutamate release. Neuron. 2005;46:275–83.
30. Pascual O, Casper KB, Kubera C, Zhang J, Revilla-Sanchez R, Sul JY, et al. Astrocytic purinergic signaling coordinates synaptic networks. Science. 2005;310:113–6.
31. Courjaret R, Tröger M, Deitmer JW. Suppression of GABA input by A1 adenosine receptor activation in rat cerebellar granule cells. Neurosci. 2009;162:946–58.
32. Tabata T, Kawakami D, Hashimoto K, Kassai H, Yoshida T, Hashimotodani Y, et al. G protein-independent neuromodulatory action of adenosine on metabotropic glutamate signaling in mouse cerebellar Purkinje cells. J Physiol. 2007;581:693–708.
33. Patel SC, Suresh S, Kumar U, Hu CY, Cooney A, Blanchette-Mackie EJ, et al. Localization of Niemann–Pick C1 protein in astrocytes: Implications for neuronal degeneration in Niemann–Pick type C disease. Proc Natl Acad Sci USA. 1999;96:1657–62.
34. Chen G, Li HM, Chen YR, Gu XS, Duan S. Decreased estradiol release from astrocytes contributes to the neurodegeneration ina mouse model of Niemann–Pick disease type C. Glia. 2007;55:1509–18.
35. Dunwiddie TV, Diao L, Proctor WR. Adenine nucleotides undergo rapid, quantitative conversion to adenosine in the extracellular space in rat hippocampus. J Neurosci. 1997;17:7673–82.
36. Atterbury A, Wall MJ. Adenosine signalling at immature parallel fibre-Purkinje cell synapses in rat cerebellum. J Physiol. 2009;587:4497–508.
37. Zhou SY, Xu SJ, Yan YG, Yu HM, Ling SC, Luo JH. Decreased purinergic inhibition of synaptic activity in a mouse model of Niemann–Pick disease type C. Hippocampus. 2010. doi:10.1002/hipo.20741.